POLITECNICO DI TORINO
Repository ISTITUZIONALE

Clipping and Quantization Impact in Power-Imbalanced Upstream DSCM Coherent PONs

Original
Clipping and Quantization Impact in Power-Imbalanced Upstream DSCM Coherent PONs / Al Zoubi, S., Gaudino, R.. - (In corso di stampa). (2026 26th International Conference on Transparent Optical Networks (ICTON) Prague (Cze) 12-16 July 2026).

Availability:
This version is available at: 11583/3013807 since: 2026-07-31T12:27:20Z

Publisher:
IEEE

Published
DOI:

Terms of use:

This article is made available under terms and conditions as specified in the corresponding bibliographic description in the repository

Publisher copyright
IEEE postprint/Author's Accepted Manuscript

©9999 IEEE. Personal use of this material is permitted. Permission from IEEE must be obtained for all other uses, in any current or future media, including reprinting/republishing this material for advertising or promotional purposes, creating new collecting works, for resale or lists, or reuse of any copyrighted component of this work in other works.

(Article begins on next page)

11 November 2026

Clipping and Quantization Impact in Power-Imbalanced Upstream DSCM Coherent PONs

Safana Alzoubi[1,*] and Roberto Gaudino[1]
[1]Dipartimento di Elettronica e Telecomunicazioni, Politecnico di Torino, Torino, Italy. *safana.alzoubi@polito.it

***Abstract*—Future passive optical networks (PONs) are targeting data rates of 200 Gbps/λ and beyond, while moving toward end-to-end coherent transmission from metro to access networks. In this context, deploying digital subcarrier multiplexing (DSCM) is attractive for enabling low-latency and high-flexibility services, such as 5G/6G fronthauling. DSCM offers finer granularity in bit-rate allocation compared to single-carrier coherent solution. However, adapting coherent transmission in general, and DSCM in particular, to the shared PON infrastructure is challenging due to several constraints, including the wide dynamic range in upstream transmission. Additionally, the multi-carrier nature of DSCM increases the peak values relative to the signal average in the Tx and Rx electrical signals, and thus higher penalties are exhibited in systems with low-resolution analog-to-digital converters (ADCs). This penalty further increases when considering the inherent power imbalance in PON architectures, making it a critical limitation in DSCM-PON performance that must be carefully considered in physical-layer design and network planning. In this context, clipping can be employed to mitigate high signal peaks, but it must be carefully optimized to balance clipping and quantization penalties. Therefore, this paper investigates the impact of subcarrier power imbalance on the performance of upstream DSCM coherent PON, with a particular focus on clipping and quantization effects introduced by finite-resolution ADCs.**

***Index Terms*—Coherent passive optical network (PON), digital sub-carrier multiplexing (DSCM), power imbalance.**

I. Introduction

Future passive optical networks are anticipated to deliver data rates beyond 200 Gbps per wavelength to support the high data rate demands of 5G/6G x-hauling services [1], while also accommodating high optical distribution losses, providing greater flexibility, and enabling coexistence with legacy and other services such as analog radio-over-fiber [2]. In response to these requirements, a working group within the International Telecommunication Union (ITU-T) is leading the Very High Speed PON (VHSP) initiative to evaluate technical options for next-generation PON systems [3]. In this direction, coherent transmission and its digital subcarrier multiplexing (DSCM) variant are being investigated as promising candidate technologies for future PON deployments [4], [5]. Coherent transmission utilize amplitude, phase, and polarization and even more its variant DSCM improves flexibility in bit-rate per subcarrier, while enabling the use of lower-bandwidth optical network units (ONUs) [6]. Furthermore, DSCM-based coherent PON can provide lower latency by assigning dedicated subcarriers to ONUs, compared to its counterpart single-carrier coherent.

Although DSCM has been widely studied in point-to-point systems, its deployment in point-to-multipoint PONs remains challenging due to additional system constraints [7]. These include upstream burst-mode operation, laser control in ONUs, and the large power dynamic range in PON systems, which can reach up to 20 dB at the optical line terminal (OLT) upstream receiver (RX). Conventionally, power dynamics in burst time-division multiplexing (TDM)-PON are controlled via automatic gain control (AGC) in the transimpedance amplifier (TIA). In DSCM, however, this becomes more challenging due to the additional mixing of subcarriers (SCs) in the time domain. As a result, careful SC planning and pre-leveling of the ONU transmitted power are required [8]. This is particularly important since SC power imbalance (PI) can interact with other impairments, including clipping and quantization, laser frequency offset, fiber nonlinearities and others.

In this context, the large dynamic range in DSCM-PON systems makes multicarrier-related impairments particularly relevant, such as peak-to-average power ratio (PAPR), which is a well-known challenge arising from the addition of SCs in the time domain, leading to performance degradation in the presence of nonlinearities and limited-resolution quantization in analog-to-digital converter (ADC). To control the resulting signal dynamic range, electrical signal clipping is one of the proposed methods employed to reduce signal peaks and consequently the required quantization range. These impairments have been widely studied in the literature, particularly in orthogonal frequency division multiplexing (OFDM) systems for both wireless and optical applications [9]. However, they remain less explored in optical DSCM systems with scarce work on DSP-based PAPR reduction techniques [10], [11]. In DSCM-PON systems, the presence of subcarrier power imbalance further increases the effective signal dynamic range, worsening the resulting clipping and quantization penalties. Additionally, although clipping and quantization are extensively studied and modeled in conventional multicarrier systems, these models are not directly applicable to DSCM-PON. This is due to the combined effects of DSCM-PON specifications: the low number of SCs (4,8 and 16), the presence of PI between SCs, and separate clipping on the in-phase (I) and quadrature (Q) components.

Given these challenges in DSCM PON systems, this paper

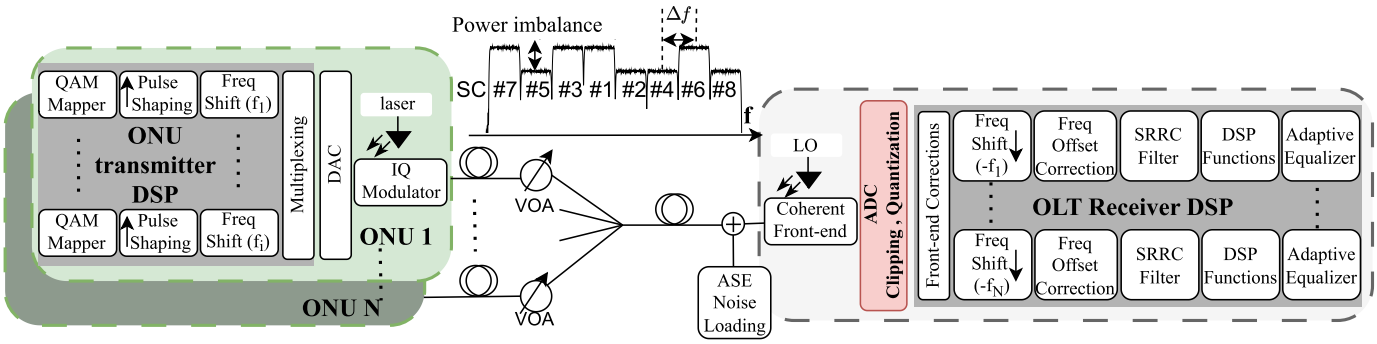

Fig. 1. Block diagram of the upstream signal processing in a DSCM PON. Inset illustrates the OLT received SCs with power imbalance. ONU: optical network unit; DAC: digital-to-analog converter; VOA: variable optical attenuator; ASE: amplified spontaneous emission; LO: local oscillator; ADC: analog-to-digital converter; OLT: optical line terminal. SRRC: square-root raised cosine.

investigates the impact of upstream PI on DSCM performance, with a particular focus on ADC impairments, namely clipping and quantization. We consider a system using only frequency division multiplexing (FDM), rather than time-frequency division multiplexing (TFDM), in order to isolate the impact of SC PI, accordingly dedicated SC groups per ONU are assumed. To evaluate these impairments, we carry out numerical simulations and study the performance degradation arising from the combined effects of SC PI, clipping, and quantization. Understanding and addressing this imbalance is important for ONU power pre-leveling, the design of physical-layer transmission specifications, mitigation strategies, and network dimensioning. Other impairments, such as TX/RX IQ imbalance, chromatic dispersion, laser phase noise, and fiber nonlinearities are not considered, as they are beyond the scope of this work.

II. Digital Subcarrier Multiplexed PON System

Figure 1 illustrates the ONU transmitters and the OLT receiver, highlighting the upstream signal processing in a DSCM coherent PON. We consider a system with M SCs, where ONUs are assigned distinct SCs. Each ONU generates complex baseband QAM-modulated signals at a symbol rate of R_s, which are Nyquist pulse-shaped using a square-root raised cosine (SRRC) filter with a roll-off factor ρ. The signals are then frequency up-shifted to their respective SC center frequencies, with spacing defined as $\Delta f = R_s(1+\rho)$, as depicted in the SC inset in Fig. 1. The SCs are subsequently multiplexed in DSP, converted to analog through a digital-to-analog converter, followed by the optical IQ modulator. Signals from different ONUs, occupying distinct SCs, propagate through separate fiber paths with varying lengths and losses, before being combined via passive power splitters and transmitted over the shared fiber. At the OLT receiver, the received optical signal is loaded with amplified spontaneous emission (ASE) noise. Some examples of the resulting spectra are given in Fig. 2. It was demonstrated that, for coherent receivers, the internal electrical noise is also additive Gaussian, and thus has the same impact as ASE (as discussed later). Although optical amplification is not typically used in coherent PON systems, it may be introduced to increase the power budget such as in [8]. At the OLT receiver side, the received optical signal is first coherently detected and then the four resulting electrical signals are passed through the 4 ADCs, where clipping and quantization are applied before receiver DSP. Clipping is characterized by a symmetric threshold A such that

$$x_c = \begin{cases} A & x > A \\ x & -A \le x \le A \\ -A & x < -A, \end{cases} \tag{1}$$

where x and x_c represent the input and clipped signals on each quadrature component, respectively. The clipping ratio is then defined as $\mu = A/\sigma_x$, where σ_x^2 is the variance of each of the four electrical signals at ADC inputs [12]. Quantization noise, in turn, is introduced by ADC digitization and can be considered as white and additive. This assumption is valid only for sufficiently high resolutions, i.e., when the effective number of bits (ENOB) is at least 4 bits or higher [13]. The ADC noise variance is defined as $\Delta^2/12$, where Δ is the quantization step size and equals $2A/(2^{ENOB}-1)$. Following ADCs, the DSCM signal initially undergoes front-end corrections, after which each SC is frequency down-shifted to baseband, and down-sampled to 2 samples per symbol. Each SC is then processed through the DSP chain for coherent detection, including chromatic dispersion compensation, frequency offset estimation and correction, filtering, carrier phase compensation, and adaptive equalization to recover the individual SCs.

III. Power-imbalanced DSCM Simulation Setup

This section presents the numerical simulations conducted to evaluate the combined impact of clipping and/or quantization in the presence of PI through the resulting performance degradation. The PM-16QAM DSC signals are generated according to the processing blocks shown in Fig. 1. A different pseudo-random binary sequence (PRBS) of degree 16 is used for each SC, with 10 repetitions, and the SC symbol rate is $R_s = 4$ Gbaud. The roll-off factor is 0.05 and filter length is 32, and the SC spacing follows the roll-off factor such that $\Delta f = R_s(1+\rho)$ corresponding to a total upstream line bit-rate equal to 256 and 512 Gbps for M = 8 or M = 16 SCs. A T/2-spaced 2×2 complex MIMO feed-forward equalizer is used for polarization demultiplexing and equalization on each SC. The equalizer employs the least mean square (LMS) algorithm and approximates an ideal MMSE equalization. Finally, symbol decisions are performed and the BER is calculated by counting errors per SC. Throughout the simulations, the number of

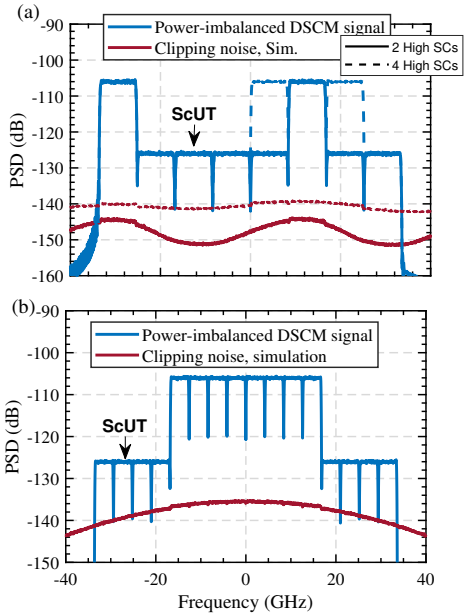

Fig. 2. Power spectral density of a DSCM signal with 20 dB of power imbalance and the corresponding clipping distortion for a clipping ratio of $\mu = 2.5$ in a system with (a) 8 SCs and (b) 16 SCs. ScUT: subcarrier under test.

SCs is varied between 8 and 16. For each case, an arbitrary subset and location of SCs is selected to experience lower loss and, consequently, higher received power compared to the remaining SCs. Figure 2 shows the power spectral density (PSD) of the received power-imbalanced DSCM signal with 20 dB power difference between the high and low power SCs. In the 8-SC case, 2 SCs and 4 SCs are set to higher power levels, as shown in (a), while for the 16-SC system, 8 SCs have higher power. The figure also illustrates in red the PSD of the clipping distortion, defined as the difference between the clipped complex signal (where the I and Q components are clipped separately with a clipping ratio of $\mu = 2.5$) and the unclipped signal, for each scenario. It can be seen that the clipping distortion is not white across the SCs, but instead follows the power distribution of the received signal. Moreover, increasing the number of high-power SCs (e.g., from 2 to 4) leads to a higher clipping distortion PSD across all SCs. The key performance metric in this work is the optical signal-to-noise ratio (OSNR) required to achieve a target BER specifically 2E-2, and the corresponding OSNR penalty induced by the considered physical-layer impairments. Despite this, it has been demonstrated in [14] that, for a non-optically amplified coherent receiver, the OSNR penalty directly translates into a received optical power (ROP) penalty in terms of sensitivity at the same BER target. Accordingly, the results presented as OSNR penalties can equivalently be interpreted as ROP penalties in such receivers.

IV. Simulation Results and Discussion

In this section, we study the OSNR penalty versus a variety of system design key parameters. We begin by presenting the OSNR penalty for an 8-SC system under different clipping ratios in Fig. 3, namely (a) no clipping, (b) clipping ratio of

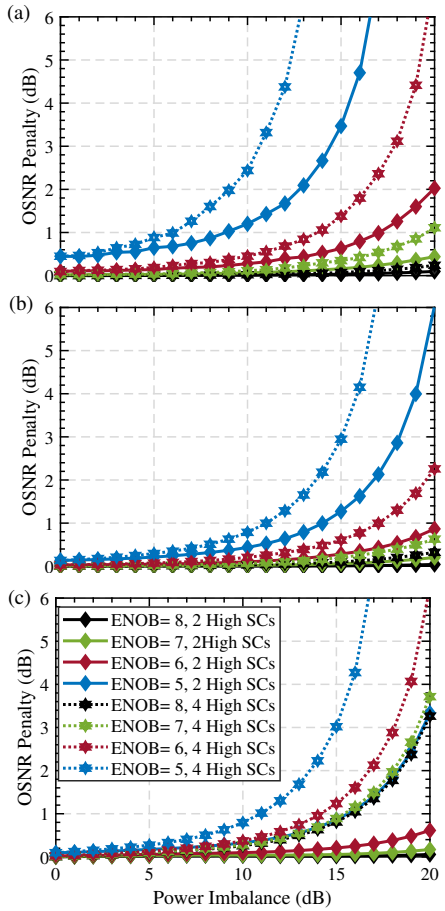

Fig. 3. Optical signal-to-noise ratio penalty versus SC power imbalance for different ADC effective numbers of bits and numbers of high-power SCs is an 8-SC system, with clipping ratios of (a) no clipping, (b) $\mu = 3$, and (c) $\mu = 2.5$. Legend of (c) applies to all SCs.

3, and (c) clipping ratio of 2.5. In this figure, the penalty is evaluated for ENOB values of 5, 6, 7, and 8, and for two scenarios with either 2 or 4 high-power SCs. The following analysis studies the OSNR penalty for the SCs indicated in Fig. 2 as SC under test (ScUT). The selected SCs are chosen to be non-adjacent to high-power SCs in order to isolate the impact of clipping and quantization from other effects, such as inter-subcarrier interference arising from non-ideal SRRC filtering for example. Nevertheless, future work should investigate clipping and quantization effects across all SCs, including the combined impact of ADC limitations and other impairments. As seen in Fig. 3, increasing the PI between SCs leads to a higher OSNR penalty for the ScUT; however, this degradation is more significant for low-resolution ADCs (ENOB = 5), reaching values above 1 dB for 2 high SCs and PI values of 10 dB without clipping, or 15 dB PI with clipping. In contrast, this penalty becomes negligible for higher-resolution ADCs (ENOB = 7 and 8). Increasing the number of high-power SCs further exacerbates the OSNR penalty, as the dashed curves consistently exhibit higher penalties than their solid counterparts. Moreover, the gap between the 2 and 4 high-SC scenarios increases with lower ADC resolution. This can be attributed to the increased signal dynamic range combined with the limited resolution of the ADC. Applying

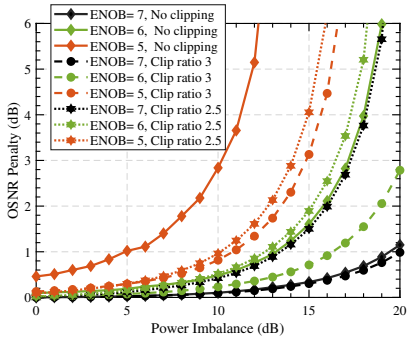

Fig. 4. Optical signal-to-noise ratio penalty versus SC power imbalance for different effective numbers of bits and clipping ratios in a 16-SC setup with 8 high SCs.

clipping with a ratio of 3 improves performance compared to the no-clipping case across all ENOB values and power distributions. For example, at a PI of 15 dB, the penalty is reduced from more than 6 dB to approximately 3 dB, and from more than 3 dB to about 1 dB for ENOB = 5 with 4 and 2 high-power SCs, respectively. Reducing the clipping ratio further from 3 to 2.5 provides additional noticeable improvement only for ENOB = 5 when the number of high-power SCs is 2. However, it degrades performance for higher ENOB values (6–8) and when 4 SCs have high power. This indicates that the optimal clipping ratio depends on multiple factors, including the power distribution among SCs, the clipping level, and the ADC resolution.

Next, we evaluate the OSNR penalty for a 16-SC system with 8 high-power SCs in Fig. 4 for various clipping ratios. Similar to the 8-SC case, the OSNR penalty increases with PI between SCs and this penalty decreases with higher ADC resolution. The penalty can reach up to 3 dB for a 10 dB PI and more than 6 dB for a 15 dB PI for ENOB of 5 in the absence of clipping. A clipping ratio of 3 consistently outperforms both the no-clipping case and a clipping ratio of 2.5 across all ENOB values. For higher-resolution ADCs (ENOB = 6 and 7), no clipping performs better than a clipping ratio of 2.5. In contrast, for low-resolution ADCs (ENOB = 5), clipping with a ratio of 2.5 provides better performance than no clipping. These results show that, for an acceptable OSNR penalty of 1 dB in a future DSCM PON, a PI of up to 20 dB can be tolerated when the ADC resolution is ENOB $\geq$ 7 combined with optimized clipping. For lower ADC resolutions, power pre-leveling at the transmitter side is required to limit the PI to approximately 10 dB. It is also worth noting that, as suggested by the clipping noise PSD distribution, the optimal clipping ratio and SC power pre-leveling are likely SC-position dependent. Future work should investigate other SC configurations and spectral allocation strategies, such as grouping high-power SCs together, and evaluate the associated trade-offs in upstream resource allocation flexibility.

V. Conclusion

In this study, we investigated the impact of subcarrier PI on the performance of future DSCM-PON systems via numerical simulations. The goal of this work is to analyze system penalties arising from the combination of PI and non-ideal ADCs, and to support proper transceiver physical-layer design consideration, such as the ENOB required for DSCM receivers and clipping ratios. We show that PI between upstream SCs degrades system performance due to ADC impairments, particularly quantization. This degradation can exceed 6 dB within the considered parameter space and provides insight into how transmitter power should be pre-leveled. Clipping can partially mitigate this degradation, but this strongly depends on the operating conditions. Future investigations should consider modeling the interaction between clipping, quantization noise, and PI, as well as determining the optimal clipping ratio. Furthermore, the joint impact of PI with other impairments in DSCM transmission should be investigated.

Acknowledgment

This work has received funding from the European Union's Horizon Europe research and innovation programme under the Marie Skłodowska-Curie grant agreement No. 101073265 (EWOC). Views and opinions expressed are however those of the authors only and do not necessarily reflect those of the European Union. The European Union cannot be held responsible for them. The Authors are with the Politecnico di Torino PhotoNext Center for Applied Photonics.

References

[1] Z. Vujicic *et al.*, "Toward virtualized optical-wireless heterogeneous networks," *IEEE Access*, vol. 12, pp. 87776–87806, 2024.

[2] Z. Vujicic *et al.*, "On the feasibility of analog fiber dispersion-based photonic beamforming for mmWave wireless access over 100 GHz DWDM grids," *J. Opt. Commun. Netw.*, vol. 17, pp. E70–E81, Nov 2025.

[3] D. Zhang *et al.*, "Progress of very high speed PON in ITU-T," *J. Opt. Commun. Netw.*, vol. 18, no. 2, pp. A112–A122, 2026.

[4] R. Gaudino *et al.*, "Coherent PON: Recent evolutions and expected trends," in *Optical Fiber Communication Conference (OFC) 2025*, p. M2I.1, 2025.

[5] Z. Jia *et al.*, "Coherent passive optical network: Applications, technologies, and specification development," *J. Opt. Commun. Netw.*, vol. 17, no. 1, pp. A71–A86, 2025.

[6] J. Li *et al.*, "Bidirectional TFDM 200 G coherent PON with a simplified receiver at the ONU side," *Opt. Lett.*, vol. 49, no. 18, pp. 5127–5130, 2024.

[7] T. Duthel *et al.*, "DSP design for coherent optical point-to-multipoint transmission," *J. Lightwave Technol.*, vol. 42, no. 3, pp. 1109–1118, 2024.

[8] M. Xu *et al.*, "Intelligent burst receiving control in 100G coherent PON with 4×25G TFDM upstream transmission," in *Optical Fiber Communication Conference (OFC) 2022*, p. Th3E.2, 2022.

[9] C. R. Berger *et al.*, "Theoretical and experimental evaluation of clipping and quantization noise for optical OFDM," *Opt. Express*, vol. 19, no. 18, pp. 17713–17728, 2011.

[10] P. Luo *et al.*, "Low-complexity PAPR reduction based on partial transmit subcarrier technology in 400G coherent TFDM PON," in *2025 Optical Fiber Communications Conference and Exhibition (OFC)*, pp. 1–3, 2025.

[11] J. Zhang *et al.*, "PAPR reduction and nonlinearity mitigation of optical digital subcarrier multiplexing systems," *J. Lightwave Technol.*, vol. 41, no. 22, pp. 6957–6969, 2023.

[12] D. Dardari *et al.*, "Joint clip and quantization effects characterization in OFDM receivers," *IEEE Trans. Circuits Syst. I*, vol. 53, no. 8, pp. 1741–1748, 2006.

[13] A. Napoli *et al.*, "Digital compensation of bandwidth limitations for high-speed DACs and ADCs," *J. Lightwave Technol.*, vol. 34, no. 13, pp. 3053–3064, 2016.

[14] G. Rizzelli *et al.*, "Planning tools for next-generation DSP-based passive optical networks above 50G," *J. Opt. Commun. Netw.*, vol. 16, no. 7, pp. C88–C96, 2024.